

Supporting Information

Photophysics and dynamics of Surface Plasmon Polaritons mediated Energy Transfer in the presence of an applied electric field

Elisabetta Collini,*¹ Francesco Todescato,¹ Camilla Ferrante,¹ Renato Bozio,¹ Gregory D. Scholes²

¹*Department of Chemical Sciences and INSTM, University of Padova, Via Marzolo 1, I-35131 Padova, Italy.*

²*Department of Chemistry, University of Toronto, 80 St George Street, Toronto (ON) M5S3H6, Canada.*

*elisabetta.collini@unipd.it

Contents

S.1. Analysis of all possible pathways contributing to the final PL signal

Figure S1

S.2. Estimate of the excitons and hole polarons densities

S.3. Simulation of OLED outcoupling with and without the DPA layer

Figure S2

S.4. Fitting parameters for luminescence decays of EPH2 structures

Table S1

S.5. Experimental data obtained with other D/A couples

Figure S3

S.1. Analysis of all possible pathways contributing to the final PL signal

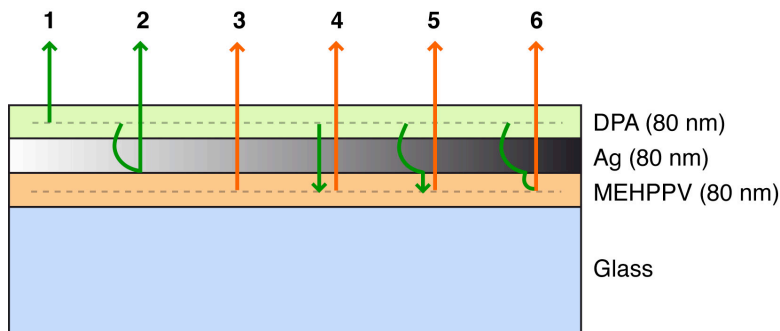


Figure S.1. Cross section of the model multilayer structure showing 6 possible pathways contributing to the final signal, following photo-excitation at 400 nm into the DPA layer: (1) direct emission from DPA; (2) SPP radiation; (3) emission from MEH-PPV directly excited; (4) trivial ET; (5) SPP radiation followed by MEH-PPV excitation; (6) SPP mediated ET. Straight (curved) lines indicate radiative (non-radiative) coupling.

Considering the geometry of the experiment (see Section 2), six main relaxation pathways following DPA excitation can be individuated, as depicted in Figure S.1:

- 1) direct emission from DPA layer.
- 2) direct SPP radiation, mediated by the surface roughness.
- 3) emission from MEH-PPV layer directly excited by the pump beam.
- 4) conventional ET from DPA to MEH-PPV.
- 5) SPP radiation promoting MEH-PPV excitation; this is the same as pathway (2), but the light emitted by SPP modes is absorbed and re-emitted by the MEH-PPV layer.
- 6) SPP-ET: energy from decaying dipoles couples into SPP modes, which then evanescently couple to the emissive MEH-PPV.

Contributions to the signal deriving from pathway (1) and (2) were minimized recording only the PL in the spectral region dominated by the emission of the acceptor MEH-PPV ($\lambda > 610$ nm), thanks to suitable long-pass filters. Analysis of donor-only sample (glass/Ag/DPA) confirmed that the residual signal due to donor PL in the adopted experimental conditions is at least 2 orders of magnitude weaker than the acceptor PL.

Although the exciting beam is focalized in the DPA layer, the axial resolution in our experimental setup is about 6 μm , thus direct excitation of MEH-PPV dipoles (pathway (3)) cannot be completely

ruled out. The contribution of this pathway is anyway minimized by the shielding effect of the Ag layer. Such contribution was verified recording the signal of control films with structure glass/MEH-PPV/Ag, as a function of metal thickness. It was verified that for metal thicknesses >60 nm there is no contribution from direct excitation of MEH-PPV, whereas for thinner thicknesses such contribution becomes increasingly more relevant (see Table 1). Even in these conditions, however, the exact contribution from this process can be easily estimated (and then subtracted) measuring the PL decay for acceptor-only samples in the same experimental conditions.

The contributions of pathways (4) and (5) are not easily distinguishable from the SPP-ET (pathway 6) in the experimental signal, but a rough estimate can be made based on simulations described in Section 3. To do that, the energy flux at the top of metal layer was integrated across the radiative and SPP range of wavevectors. For the multilayer structure, the fraction of energy transferred to SPP is about the 90% of the overall flux, so it can be predicted that the contribution of processes (4) and (5) to the final signal is negligible. For this reason, it is thus meaningful to analyze the experimental results attributing the PL signal recorded for the multilayer samples as due to the SPP-ET process.

S.2. Estimate of the excitons and hole polarons densities

The number of excitons instantaneously photogenerated in the MEH-PPV layer can be roughly estimated multiplying the efficiency of the SPP-ET (Φ_{SPP-ET}) by the number of photoexcitations initially created by the laser beam in the donor DPA layer:

$$n_{exc} = \Phi_{SPP-ET} \cdot \frac{E (1 - 10^{-Abs})}{V h\nu}$$

where E is the energy per pulse of the exciting beam, V is the excited volume, $h\nu$ is the photon energy and Abs is the absorbance of the DPA layer at 400 nm. Here it is assumed that: (a) each absorbed photon generates an excitation in the DPA layer, (b) scattering is negligible, (c) there is no direct excitation of MEH-PPV by the 400 nm beam, (d) all the excitations generated in the MEH-PPV through SPP-ET are neutral excitons and (e) the excited volume V can be approximated as a cylinder with base equal to the experimental spot size and height equal to the thickness of the MEH-PPV layer. Inserting in the equation the experimental values, a density of about 10^{15} excitons/cm³ can be calculated. From literature data [A. Rihani *et al.*, *Org. Elec.* 7, **2006**, 1 and references therein], a density of hole polarons of the same order of magnitude (10^{15} polarons/cm³ at 15V) can be estimated.

Here we consider the upper limit for the hole density in the bulk, which can be estimated by a direct calculation of the holes injected through the ITO/MEH-PPV interface as $p_{inj} \approx p_0 \exp(-\Delta/kT)$. Assuming a barrier height (Δ) of the order of about 0.3 eV [D.D.C. Bardley, *Synth. Met.* 54, **1993**, 401] and a density of states (p_0) of the order of 10^{20} cm^{-3} [A.J. Campbel *et al.*, *J. Appl. Phys.* 82, **1997**, 6326], a hole density of about 10^{15} polarons/cm³ can be calculated.

S.3. Simulation of OLED outcoupling with and without the DPA layer

The presence of the additional DPA layer with respect to the conventional OLED structure could act in different ways to cause the recorded enhancement. First, we can exclude any influence on the efficiency of charge injection from metal electrodes and of charge transport within the polymer layer, because these processes are mainly connected with the morphology of the polymer film and the nature of the interfaces with the electrodes. However, the presence of an organic layer on top of the metal cathode could in some way affect the coupling of excitons to photon states allowed in the device structure. It is now well known that the presence of the metallic cathode has the effect of reducing the radiative emission rates for polymer chains placed at the nodal spacings from the cathode, and in addition, there can be energy transfer into plasmon modes of the metal. To check if the presence of a further organic layer with $\epsilon > 1$ above the metal cathode could lead to some modification of the coupling of the MEH-PPV emission to photon states of the device, we simulated the power-dissipation spectrum of the device within the same model described in Section 3. In this case we analyzed the power dissipated by a dipole located in the emissive MEH-PPV layer. When the in-plane wave-vector of the dipole emission matches that of a mode of the structure, the dipole may resonantly lose power to that mode. Thus, peaks in the power-dissipation spectrum indicate the different modes of the structure. In panel (a) and (b) of Figure S.2, dissipation spectra as a function of in-plane wavevector are shown for an OLED without (referred as EPH1 in the main text) and with the DPA layer (EPH2), respectively. Looking at the positions of the brighter features, it is immediately noticeable that the presence of DPA layer does not modify the device modes. This is confirmed in panels (c) and (d), where the efficiency of the coupling to the different layers is depicted. This behavior was also verified experimentally comparing the EL signal from OLED with and without the DPA layer.

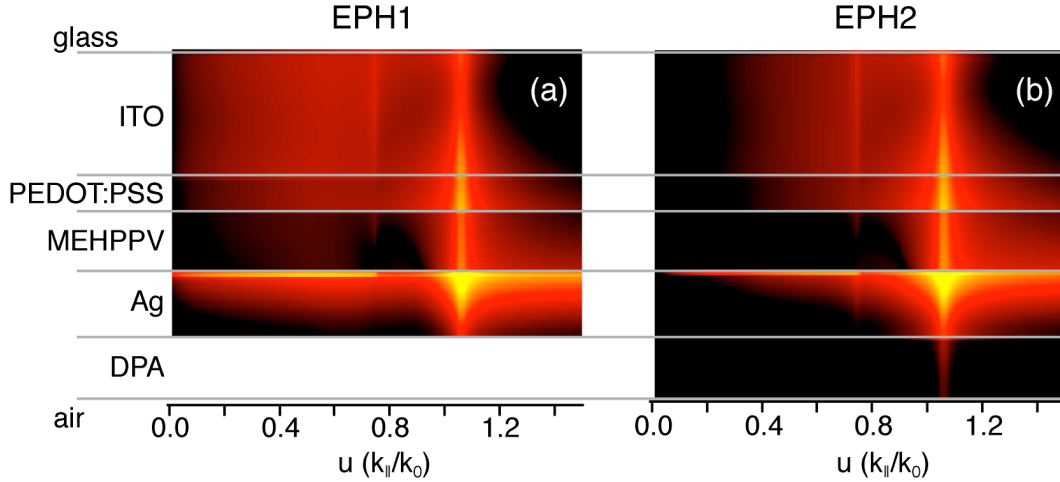


Figure S.2. Absorption of dipole energy as a function of the position and normalized surface-parallel vector for (a) EPH1 and (b) EPH2 (logarithmic color scale). In both structures the dipole is located at the middle of the MEH-PPV emissive layer and the emission wavelength is 500 nm. Bright features correspond to higher absorption.

S.4. Fitting parameters for luminescence decays of EPH2 structures

Table S1 summarizes the fitting parameters of the luminescence decays at different values of applied bias for the EPH2 of Figure 5. In the text, the same parameters are illustrated in Figure 6(b) and 6(c). The fitting function was a sum of three exponential plus an offset (y_0), convoluted with the instrument response function (IRF). The offset y_0 has been introduced to account for the continuous contribution of electroluminescence. Deconvolution of the experimental decays from the IRF is a necessary procedure to appreciate time constants faster than the experimental resolution down to 50 ps. Note the error associated with this fast component (t_1) is bigger than for the other time constants. This anyway does not affect the discussion, since the trend of the rise component, observed as a function of the applied bias, is clearly distinguishable despite the exact value of the relative time constant.

Table S1. Fitting parameters of the luminescence decay for the EPH2 of Figure 5 and 6.

bias (V)	y_0^\ddagger	A_1	t_1 (ps)*	A_2	t_2 (ns)	A_3	t_3 (ns)
11	99	-1.91E+03	121	1.20E+03	0.89	7.2E+02	2.9
13	111	-3.11E+03	83	1.96E+03	0.72	6.5E+02	2.9
15	135	-3.82E+03	72	2.23E+03	0.51	7.8E+02	2.1
17	129	-2.38E+03	53	1.82E+03	0.45	5.3E+02	1.8
20	127	-1.25E+03	<50	1.39E+03	0.31	4.0E+02	1.3

‡ offset accounting for the continuous contribution of electroluminescence.

* obtained through deconvolution methods.

S.5. Experimental data obtained with other D/A couples.

Other combinations of dyes different from MEH-PPV/DPA were considered. Owing that the final goal was to characterize the effect of an applied electric field on the SPP-ET, we decided to employ always MEH-PPV as one of the energy transfer partners, since it is a fundamental ingredient to realize a prototype electrically pumped heterostructure. We then evaluated a number of possible dyes with suitable optical properties to act as donors for MEH-PPV in an EET process. Besides MEH-PPV/Ag/DPA, we also prepared multilayer samples where the DPA layer was replaced by (i) 9,10-dichloroanthracene (DCA), (ii) rubrene and (iii) poly(9,9-dioctylfluorenyl-2,7-diyl) (PFO). In the first case, it was not possible to obtain homogeneous layers of DCA, neither by thermal evaporation nor by drop- or spin-cast techniques from solution. The TRPL traces recorded on different points were thus not reproducible. Rubrene (case ii), although easily processable, was nevertheless characterized by an emission spectrum in film very similar to the one of MEH-PPV, making the analysis of the final PL and the calculation of EET efficiency quite challenging. In the case of PFO, it was instead possible to obtain good multilayer samples and perform TRPL measurements. In Figure S.3 the results obtained for a sample: glass/MEH-PPV/Ag (100nm)/PFO are reported.

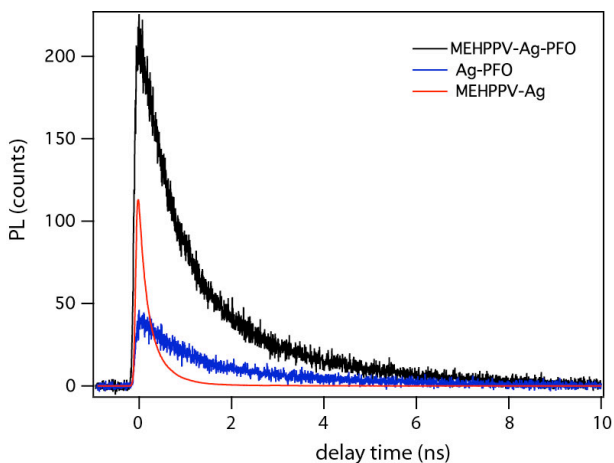


Figure S.3. Time resolved PL of a multilayer sample MEHPPV/Ag/PFO with an Ag thickness of 100 nm measured in the spectral region dominated by MEH-PPV emission ($\lambda > 610$ nm). The decay recorded for the donor-acceptor MEH-PPV/Ag/PFO film (black line) is reported together with the control samples containing donor-only (Ag/PFO, blue line) and acceptor-only (MEH-PPV/Ag, red line). The efficiency of the SPP-ET, calculated in terms of fraction of the total emission due to SPP-ET (F_{ET} , see main text), is estimated to be $63 \pm 7\%$.

As shown in the figure, the results obtained with the pair MEH-PPV/PFO looked promising, as in the case of MEH-PPV/DPA, but the PFO film resulted much more photosensitive than DPA making the measurements more difficult and less reliable.